Materials Today Advances 12 (2021) 100181

Contents lists available at ScienceDirect

Materials Today Advances

journal homepage: www.journals.elsevier.com/materials-today-advances/

Facile, clean and rapid exfoliation of boron-nitride using a non-thermal plasma process

Rodrigo F.B. de Souza, Victoria A. Maia, Priscilla.J. Zambiazzi, Larissa Otubo, Dolores R.R. Lazar, Almir O. Neto*

Instituto de Pesquisas Energéticas e Nucleares, IPEN/CNEN-SP, Av. Prof. Lineu Prestes, 2242 Cidade Universitária, CEP, 05508-000, São Paulo, Brazil

ARTICLE INFO

Article history:
Received 19 August 2021
Received in revised form
18 October 2021
Accepted 20 October 2021
Available online xxx

Keywords:
Hexagonal-boron nitride
Non-thermal plasma exfoliation

ABSTRACT

Non-Thermal Plasma source was used in this work to exfoliated boron-nitride (BN) powders. The generation of hexagonal BN nanosheets (h-BNNSs) few-layered was observed by TEM. The hBN exfoliation occurred along their transverse axis, preserving the hexagonal structure. The micrographs showed ordered lattice fringes with *d*-spacing of approximately 0.33 nm indicating the increase of (0 0 2) h-BNNSs crystal lattice planes, also confirmed by the relative peak intensity decrease in relation to the other peaks in XRD measures. The few amounts of layers were confirmed by intensity decrease, enlargement, and blue shift of $E_{2\ g}$ vibrational mode in Raman spectra. Moreover, the appearance of the FTIR band corresponding to the hydroxyl group occurs due to large amounts of defects such as vacancy defects.

1. Introduction

The exfoliation of 2D materials leads to a variety of new materials with defined shapes, preserving and even increasing their degree of crystallinity. Exfoliation methods on an industrial scale are of great interest to produce two-dimensional crystals of high quality and purity, endowed with fundamental electrical and mechanical properties for applications of energy interest [1,2]. Hexagonal boron nitride nanosheets (h-BNNSs) were first synthesized in 2004, immediately after the 2D graphene preparation by adhesive tape exfoliation [3]. The structural similarity between them attracted this attention, as boron and nitrogen atoms are arranged in a honeycomb lattice which layers are bonded by van der Waals forces. However, the exfoliation of hexagonal boron nitride (hBN) is a great challenge due to the partially ionic properties of the interlayer bonds [4].

Despite this difficulty, several BN exfoliation techniques have been explored in the literature [5–7], resulting in the obtainment of nanoparticles of different shapes, aggregating BN nanoparticles present high surface area, good chemical stability, high thermal conductivity, good biocompatibility, remarkable mechanical strength, outstanding oxidation resistance at high temperature and electronic insulation, making it a material with potential thermal properties for heat dissipation in high-performance electronic [8–10].

The present investigation provides a fast and promising technique that involves the use of a non-thermal plasma (NTP) generator used for boron nitride exfoliation. NTP is characterized by high electron temperatures and low ion temperatures in a condition of non-equilibrium which can occur at mild conditions, making this technology affordable for many industrial processes, including nanomaterials synthesis [11]. This method allows us to obtain ultrathin BN nanosheets without destroying their hexagonal crystal structure. This work, where the h-BN nanosheets were produced by a non-thermal plasma generator and characterized by a series of techniques to evaluated structural and crystalline properties.

2. Materials and methods

The scheme of the non-thermal plasma generator employed in this study is shown in Fig. 1. The experiments were carried out in a glass v-tube with an inner diameter of 10 mm. The distance between the electrodes (stainless steel) was 22 mm. A quantity of hexagonal boron nitride (h-BN) ~1 μm, 98% Sigma-Aldrich, was placed in the reactor and the exfoliation by a non-thermal plasma process started purging N_2 for 60 min.

The morphology of exfoliated material was characterized by transmission electron microscopy (TEM, Jeol JEM-2100 electron microscope, operating at 200 kV). The X-ray diffraction (XRD)

* Corresponding author.
E-mail address: aolivei@usp.br (A.O. Neto).

https://doi.org/10.1016/j.mtadv.2021.100181

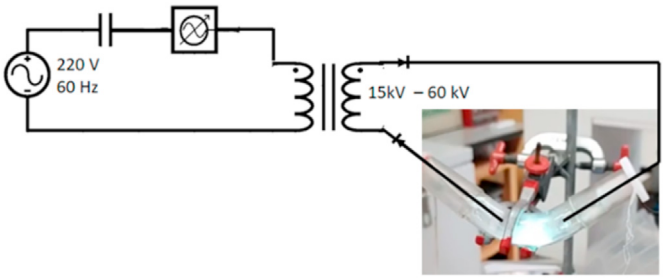

Fig. 1. Non-thermal plasma reactor system with AC high-voltage power supply, frequency/phase controller, and the reactor.

patterns were obtained using a diffractometer model Miniflex II, with Cu kα radiation source of 0.15406 Å, set at 2θ range 20–90°, with 2° min^{-1} scan speed. The Raman spectra were collected using Horiba Scientific MacroRam Raman spectroscopy equipment with laser 785 nm. The ATR-FTIR analysis was performed on an ATR accessory (MIRacle with a ZnSe Crystal Plate Pike®) installed on a Nicolet® 6700 FT-IR spectrometer equipped with a cooled MCT detector with N_2 liquid.

3. Results and discussion

The TEM micrographs of nanostructure exfoliated h-BNNSs are shown in Fig. 2a–e. Fig. 2a depicts that the exfoliation process results in a semi-transparent layered BN with ultra-thin nanosheet shapes, with an average diameter of 119.0 nm ± 44.5 nm, considering the largest length of the particles. Furthermore, the BN nanoparticles highlighted in Fig. 2a show the cross-view of the nanosheets, indicating their very thin thickness. A high-resolution image of the h-BNNSs (Fig. 2b) reveals their crystalline structure and confirms that the hexagonal structure of the starting material was well preserved, as indicates by the indexation of BN crystalline planes in the fast Fourier transformed (FFT) of this image is presented in the inset in Fig. 2c. Furthermore, the exfoliated h-BNNSs nanostructure in Fig. 2d–e presents ordered lattice fringes with *d*-spacing of approximately 0.33 nm of the (0 0 2) BN crystal lattice planes, consistent with the XRD powder analysis and with data reported in the literature [12,13].

XRD patterns of the exfoliated h-BNNSs, and of BN raw powder (Fig. 3a) show diffraction peaks at 26.7°, 41.6°, 43.7°, 54.9°, 76°, and 82.2° corresponding to the (0 0 2), (1 0 0), (1 0 1), (1 0 2), (0 0 4), (1 1 0), and (1 1 2) planes of the hexagonal phase of BN powder (JCPDS card 34–0421), respectively. It is noted that the (0 0 2) peak of exfoliated h-BNNSs presents a relative decrease in intensity in relation to the others. This behavior is highlighted in Fig. 3b as well

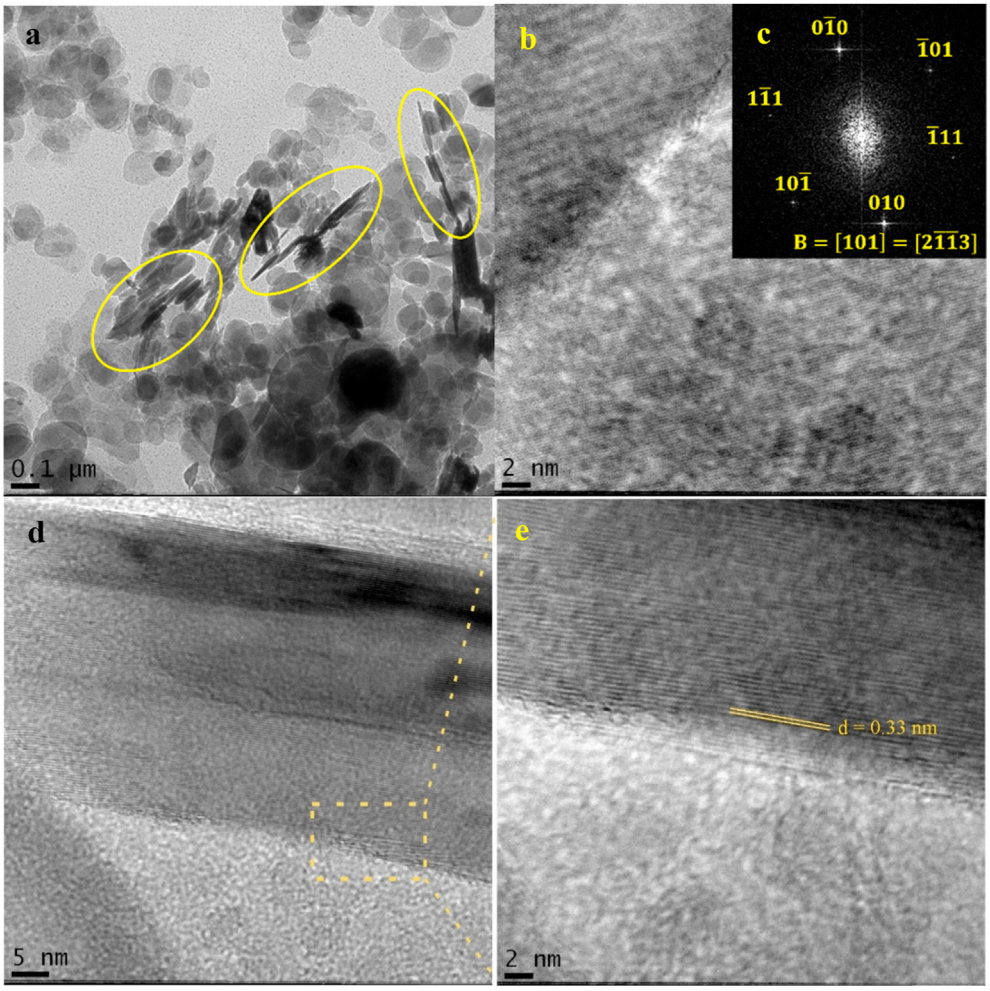

Fig. 2. TEM images of exfoliated h-BNNSs: a) ultrathin (highlighted: cross view of the nanosheets); b) high-resolution image; c) FFT of (b) image showing BN crystalline plane indexation; d-e) high-resolution images of the h-BNNSs cross view, highlighted the ordered lattice fringes with *d*-spacing 0.33 nm.

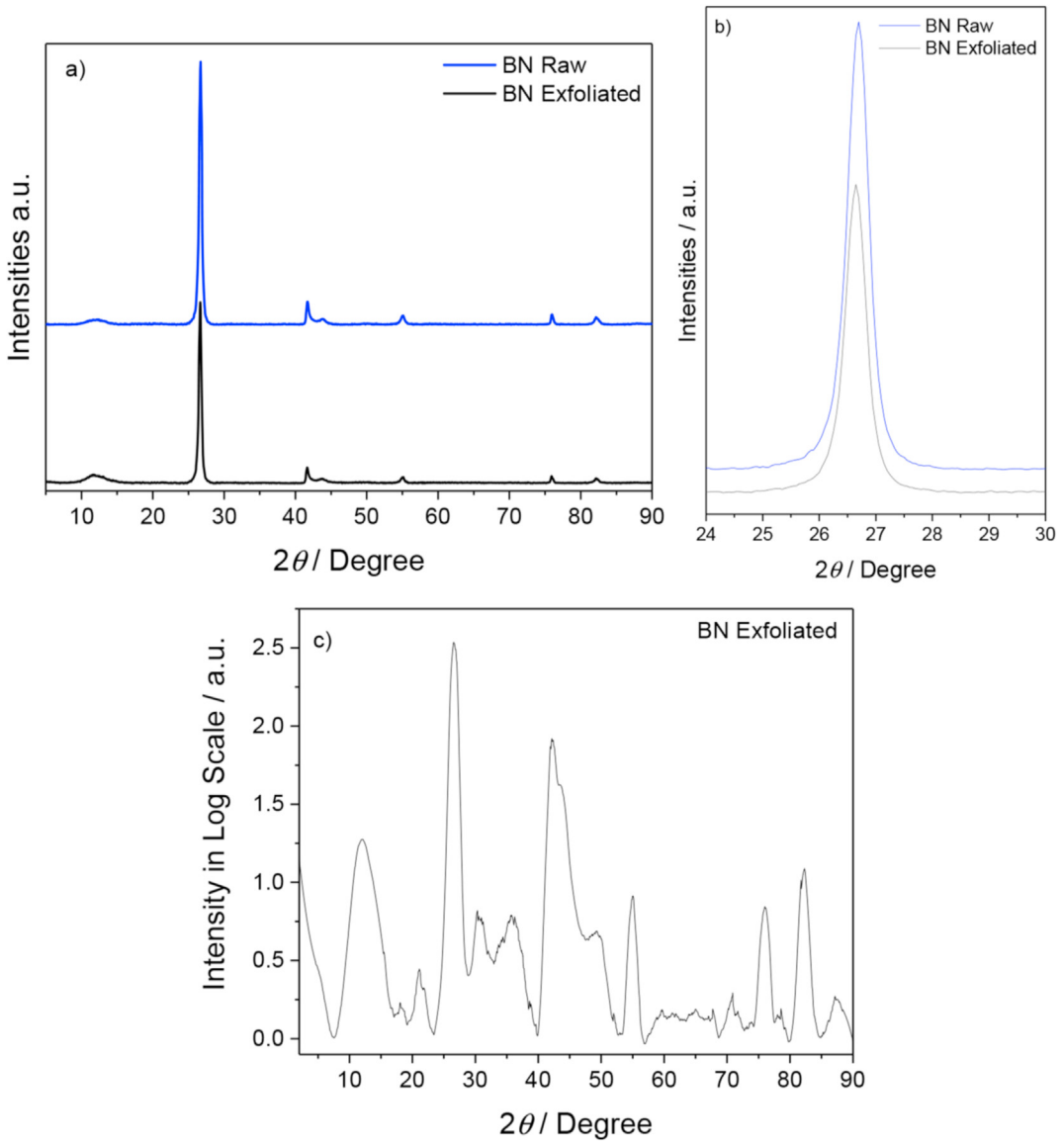

Fig. 3. X-ray diffraction a) patterns of BN Raw and h-BNNSs exfoliated; b) peak (0 0 2) detail; c) XDR plotted in logarithmic scale.

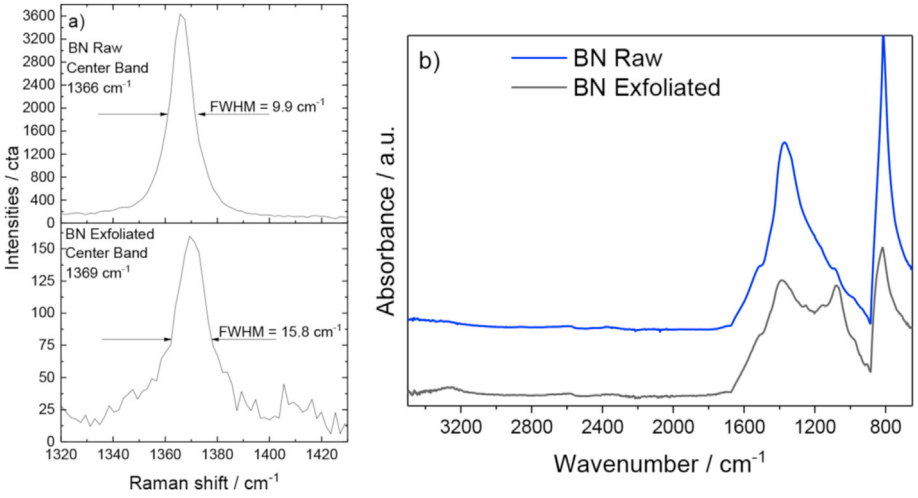

Fig. 4. a) Raman and b) FTIR spectra of BN raw and exfoliated h-BNNSs.

as a ~0.1° shift to lower 2θ. According to Zhu et al. [14], this suggests the expansion of an interplanar distance for (0 0 2) and the exfoliation in the *c* direction. Furthermore, the diffraction pattern analysis of h-BNNSs, using Bragg's Law, allows the determination of interlayer distance value of about 0.3343 nm. In addition, the crystallites dimension (L_{hkl}) was calculated using the Scherrer equation [15], and the thickness value is found as 1.703 nm for the plane (0 0 2). These values are consistent with those previously reported [2]. In Fig. 3c to investigate the h-BN obtained in more detail, the XRD pattern was plotted in logarithmic scale, where it is possible to observe beyond the faces of h-BNNSs, also peaks related to the cubic phase of boron nitride in 2 θ = ~19° (1 1 1), 31° (2 2 2), 36° (3 1 1) and 65° (4 4 0) as a reported in JCPDS # 51–779.

In the Raman spectra (Fig. 4a) it is possible to see a band centered at ~1366 cm^{-1}, corresponding to the in-plane E_{2g} vibrational mode of BN. For the raw BN the high intensity of the single peak indicates low lattice stress and high purity [16]. For the exfoliated BN there was a significant decrease in intensity, a blue shift of 4 cm^{-1}, and a FWHM of 15.8 cm^{-1} was measured, which is wider than the starting material. These factors indicate that these structures are composed of few layers, as the weaker interaction between few layers due to the exfoliation process, hardens the E_{2g} phonon mode, as suggested in the literature [17,18].

From FTIR spectra (Fig. 4b) it is possible to observe the two main characteristic bands of h-BN at ~1370 cm^{-1} and ~817 cm^{-1} B–N stretching vibration (E_{1u} mode) and out-of-plane bending vibration (A_{2u} mode), respectively [19]. Furthermore, these bands present a blue shift after the exfoliation process, as reported by Cheng and co-workers [19]. The exfoliation process revealed a band around 1075 cm^{-1} is due to the Restrahlen band of sp^3-bonded cubic-BN [20], corroborating it was observed in Fig. 3c. This band, presented as a weak shoulder of the ~1370 cm^{-1} band in BN-raw, was probably more visible on exfoliated h-BNNSs due to the blue shift of the 1390 cm^{-1} band. Perhaps the high energy involved in the exfoliation process may have favored the appearance of some trace of the cubic phase of boron nitride. In BN exfoliated a little band at ~3268 cm^{-1} corresponding to a hydroxyl group (-OH), that appears due to large amounts of defects such as vacancy defects [21,22].

4. Conclusion

In summary, the application of a non-thermal plasma reactor for boron-nitride exfoliation was effective to produce few-layered hexagonal boron nitride nanosheets (h-BNNSs). TEM images showed that the h-BNNSs, it was exfoliated along their transverse axis, preserving the hexagonal crystal structure. It was observed ordered lattice fringes with *d*-spacing of approximately 0.33 nm, indicating the increase of (0 0 2) BN crystal lattice planes, confirmed by the peak's relative intensity decrease in relation to the other peaks by XRD measures. The Raman and FTIR spectra indicated the reduction of layers by intensity decrease, enlargement, and blue shift of $E_{2\ g}$ vibrational mode in Raman spectra, and the appearance of hydroxyl band in FTIR spectra, that appear due to large amounts of defects such as vacancy defects.

Credit author statement

R.F.B. de Souza: Preparation, execution and discussion of Raman, XRD and TEM experiments; Preparation, creation and/or presentation of the published work, specifically writing the initial draft; planning and execution research. Management and coordination for the research activity planning and execution. Victoria A. Maia: Preparation and characterization experiments; preparation of hexagonal BN nanosheets (h-BNNSs). Priscilla J. Zambiazzi: Preparation, execution and discussion of Raman. Larissa Otubo: Preparation, execution and discussion of TEM experiments. Dolores R.R. Lazar: Preparation, creation and presentation of the published work writing the finally draft. Almir Oliveira Neto: Management and coordination responsibility for the research activity planning and execution; Oversight and leadership responsibility for the research activity planning and execution.

Declaration of competing interest

The authors declare that they have no known competing financial interests or personal relationships that could have appeared to influence the work reported in this paper.

Acknowledgment

We are grateful to CAPES, CNPq (302709/2020–7), FAPESP (2014/09087–4, 2014/50279–4 and 2017/11937–4) and CINE-SHELL (ANP)/FAPESP grants 2017/11937–4 for financial supports.

References

[1] D. Pan, F. Su, H. Liu, Y. Ma, R. Das, Q. Hu, C. Liu, Z. Guo, The properties and preparation methods of different boron nitride nanostructures and applications of related nanocomposites, Chem. Rec. 20 (11) (2020) 1314–1337, https://doi.org/10.1002/tcr.202000079.
[2] T. Kondo, Recent progress in boron nanomaterials, Sci. Technol. Adv. Mater. 18 (1) (2017) 780–804, https://doi.org/10.1080/14686996.2017.1379856.
[3] M. Corso, W. Auwärter, M. Muntwiler, A. Tamai, T. Greber, J. Osterwalder, Boron nitride nanomesh, Science 303 (5655) (2004) 217, https://doi.org/10.1126/science.1091979.
[4] X. Hou, Z. Yu, K.-C. Chou, Facile synthesis of hexagonal boron nitride fibers with uniform morphology, Ceram. Int. 39 (6) (2013) 6427–6431, https://doi.org/10.1016/j.ceramint.2013.01.070.
[5] S. Eshon, W. Zhang, M. Saunders, Y. Zhang, H.T. Chua, J.M. Gordon, Panorama of boron nitride nanostructures via lamp ablation, Nano Research 12 (3) (2019) 557–562, https://doi.org/10.1007/s12274-018-2252-0.
[6] Z.J. Qi, S.J. Hong, J.A. Rodríguez-Manzo, N.J. Kybert, R. Gudibande, M. Drndić, Y.W. Park, A.T.C. Johnson, Electronic transport in heterostructures of chemical vapor deposited graphene and hexagonal boron nitride, Small 11 (12) (2015) 1402–1408, https://doi.org/10.1002/smll.201402543.
[7] K.K. Kim, A. Hsu, X. Jia, S.M. Kim, Y. Shi, M. Dresselhaus, T. Palacios, J. Kong, Synthesis and characterization of hexagonal boron nitride film as a dielectric layer for graphene devices, ACS Nano 6 (10) (2012) 8583–8590, https://doi.org/10.1021/nn301675f.
[8] J. Yin, J. Li, Y. Hang, J. Yu, G. Tai, X. Li, Z. Zhang, W. Guo, Boron nitride nanostructures: fabrication, functionalization and applications, Small 12 (22) (2016) 2942–2968, https://doi.org/10.1002/smll.201600053.
[9] C. Bai, L. An, J. Zhang, X. Zhang, B. Zhang, L. Qiang, Y. Yu, J. Zhang, Superlow friction of amorphous diamond-like carbon films in humid ambient enabled by hexagonal boron nitride nanosheet wrapped carbon nanoparticles, Chem. Eng. J. 402 (2020) 126206, https://doi.org/10.1016/j.cej.2020.126206.
[10] Y. Bai, J. Zhang, Y. Wang, Z. Cao, L. An, B. Zhang, Y. Yu, J. Zhang, C. Wang, Ball milling of hexagonal boron nitride microflakes in ammonia fluoride solution gives fluorinated nanosheets that serve as effective water-dispersible lubricant additives, ACS Applied Nano Materials 2 (5) (2019) 3187–3195, https://doi.org/10.1021/acsanm.9b00502.
[11] S. Samal, Thermal plasma technology: the prospective future in material processing, J. Clean. Prod. 142 (2017) 3131–3150, https://doi.org/10.1016/j.jclepro.2016.10.154.
[12] V. Guerra, C. Wan, V. Degirmenci, J. Sloan, D. Presvytis, T. McNally, 2D boron nitride nanosheets (BNNS) prepared by high-pressure homogenisation: structure and morphology, Nanoscale 10 (41) (2018) 19469–19477, https://doi.org/10.1039/C8NR06429F.
[13] P. Singla, N. Goel, V. kumar, S. Singhal, Boron nitride nanomaterials with different morphologies: synthesis, characterization and efficient application in dye adsorption, Ceram. Int. 41 (9, Part A) (2015) 10565–10577, https://doi.org/10.1016/j.ceramint.2015.04.151.
[14] W. Zhu, X. Gao, Q. Li, H. Li, Y. Chao, M. Li, S.M. Mahurin, H. Li, H. Zhu, S. Dai, Controlled gas exfoliation of boron nitride into few-layered nanosheets, Angew. Chem. Int. Ed. 55 (36) (2016) 10766–10770, https://doi.org/10.1002/anie.201605515.
[15] A.S. Nazarov, V.N. Demin, E.D. Grayfer, A.I. Bulavchenko, A.T. Arymbaeva, H.-J. Shin, J.-Y. Choi, V.E. Fedorov, Functionalization and dispersion of hexagonal boron nitride (h-BN) nanosheets treated with inorganic reagents, Chem. Asian J. 7 (3) (2012) 554–560, https://doi.org/10.1002/asia.201100710.
[16] T.B. Hoffman, B. Clubine, Y. Zhang, K. Snow, J.H. Edgar, Optimization of Ni–Cr flux growth for hexagonal boron nitride single crystals, J. Cryst. Growth 393

(2014) 114–118, https://doi.org/10.1016/j.jcrysgro.2013.09.030.
[17] R.V. Gorbachev, I. Riaz, R.R. Nair, R. Jalil, L. Britnell, B.D. Belle, E.W. Hill, K.S. Novoselov, K. Watanabe, T. Taniguchi, A.K. Geim, P. Blake, Hunting for monolayer boron nitride: optical and Raman signatures, Small 7 (4) (2011) 465–468, https://doi.org/10.1002/smll.201001628.
[18] J. Shang, F. Xue, C. Fan, E. Ding, Preparation of few layers hexagonal boron nitride nanosheets via high-pressure homogenization, Mater. Lett. 181 (2016) 144–147, https://doi.org/10.1016/j.matlet.2016.05.154.
[19] Z.-l. Cheng, Z.-s. Ma, H.-l. Ding, Z. Liu, Environmentally friendly, scalable exfoliation for few-layered hexagonal boron nitride nanosheets (BNNSs) by multi-time thermal expansion based on released gases, J. Mater. Chem. C 7 (46) (2019) 14701–14708, https://doi.org/10.1039/C9TC03985F.
[20] J.H.C. Yang, K. Teii, C.-C. Chang, S. Matsumoto, M. Rafailovich, Biocompatible cubic boron nitride: a noncytotoxic ultrahard material, Adv. Funct. Mater. 31 (4) (2021) 2005066, https://doi.org/10.1002/adfm.202005066.
[21] M. Li, M. Wang, X. Hou, Z. Zhan, H. Wang, H. Fu, C.-T. Lin, L. Fu, N. Jiang, J. Yu, Highly thermal conductive and electrical insulating polymer composites with boron nitride, Compos. B Eng. 184 (2020) 107746, https://doi.org/10.1016/j.compositesb.2020.107746.
[22] W. Cai, D. Zhang, B. Wang, Y. Shi, Y. Pan, J. Wang, W. Hu, Y. Hu, Scalable one-step synthesis of hydroxylated boron nitride nanosheets for obtaining multifunctional polyvinyl alcohol nanocomposite films: multi-azimuth properties improvement, Compos. Sci. Technol. 168 (2018) 74–80, https://doi.org/10.1016/j.compscitech.2018.09.004.